DOI: 10.1478/AAPP.1022A6

AAPP | Atti della Accademia Peloritana dei Pericolanti
Classe di Scienze Fisiche, Matematiche e Naturali
ISSN 1825-1242

Vol. 102, No. 2, A6 (2024)

ON THE NEED OF *AD HOC* CALIBRATION FACTORS FOR ACTIVITY MEASUREMENT OF SOLUTIONS CONTAINING RADIOACTIVE MICROSPHERES

LUCREZIA AUDITORE [ab], SILVANO GNESIN [c], ANTONIO S. ITALIANO [bd*], DANIELE PISTONE [ef] AND ERNESTO AMATO [abg]

ABSTRACT. Microspheres labelled with radioactive nuclides are widely used for TransArterial RadioEmbolization (TARE) in the treatment of patients with hepatocellular carcinoma (HCC) and/or hepatic metastases. Nowadays, three commercially available devices can be used: ^{90}Y-loaded glass (Therаspheres®, Boston Scientific, Marlborough, MA, USA) and resin microspheres (Sir-Spheres®, SIRTex medical, Woburn, MA, USA), or ^{166}Ho-microspheres (QuiremSpheres™, Quirem Medical, Deventer, The Netherlands). With reference to ^{90}Y-loaded glass and resin microspheres, recent studies (S. A. Graves *et al., J. Nucl. Med.* **23**, 1131-1135 (2022); S. Gnesin *et al., J. Nucl. Med.* **64**, 825-828 (2023)) highlighted the difference between the measured activity of commercial vials and the nominal one declared by the vendors. As discussed by L. Auditore *et al. (J. Nucl. Med.* **64**, 1471-1477 (2023)), this discrepancy can be attributed to the procedure used to measure the activity of the vials at the vendor sites and to neglect the emission of Internal Bremsstrahlung (IB) photons among the radioactive decay particles emitted by ^{90}Y. The aim of this study was to investigate, by means of Monte Carlo simulations, the causes of such discrepancies, focusing on the geometrical factors affecting the activity measurement. In this study an activity calibrator was reproduced in Monte Carlo simulation environment and the measurement of the activity of a vial containing YCl_3 or ^{90}Y-labelled microspheres was simulated. With reference to the glass microspheres, the relative difference between the signal produced by the two solutions, YCl_3 and ^{90}Y-labelled microspheres, is 23.5%. This discrepancy reduces to -1.7% if the ^{90}Y-labelled microspheres are simulated as uniformly distributed in the vial. Moreover, results indicate that the geometry of the vial affects the results reducing the discrepancy from 23.5% to 16.6%. Similar results were obtained for ^{90}Y-resin microspheres for which the discrepancy with respect to the reference solution reduces from -15% to -8.6% when considering the microspheres homogeneously dispersed in the vial. Since the activity of a device employed for therapy has to be accurately known, this study highlights the need of updating the procedure of measuring the activity of such particulate solutions by using *ad hoc* calibration factors to consider the real vial geometry and distribution of the radioactive solute in the vial.

1. Introduction

TransArterial RadioEmbolization (TARE) is a therapeutic approach for patients with HepatoCellular Carcinoma (HCC) and/or hepatic metastases, employing radionuclide-labelled microspheres, made of glass or resin (Chiesa *et al.* 2021; Levillain *et al.* 2021; Weber *et al.* 2022). The treatment is planned to optimize the dose delivered to the hepatic lesions and to the healthy tissues. This is achieved performing a patient specific pre-treatment dosimetry that is routinely done by a (^{99m}Tc)-macroaggregated albumin (MAA) Single Photon Emission Computed Tomography (SPECT), often supported also by direct Monte Carlo (MC) simulation (Auditore *et al.* 2019; Amato *et al.* 2020; Auditore *et al.* 2020, 2022; Pistone *et al.* 2022). However, the pillar for these pre-treatment studies is the accurate knowledge of the activity of radio-labelled microspheres to be injected to the patients. The potential inaccuracy of the activity measurement at the vendor site would result in direct dosimetry bias affecting the determination of reliable dose-response relations. The common procedure for activity determination uses calibration factors estimated for a YCl_3 solution uniformly distributed in a vial shaped as a hollow cylinder. However, the commercial vial used to sell ^{90}Y-loaded glass microspheres is a V-shaped vial, a very different geometry with respect to the cylindrical shape. Moreover, in a solution containing microspheres, the radioactivity is not uniformly distributed in the vial since these microparticles rapidly deposit to the bottom, leaving the rest of the vial filled with a non-radioactive solution. Consequently, for vials containing microspheres in aqueous solutions, both the geometry of the commercial vial and the (non-uniform) distribution of radioactive microspheres in the vial lead to a configuration which substantially differs from the standard homogeneous YCl_3 solution used a metrological standard, therefore, the calibration factors deduced with such a reference could be not appropriate.

With reference to yttrium-90 (^{90}Y)-loaded glass and resin microspheres, recent studies (Graves *et al.* 2022; Gnesin *et al.* 2023) highlighted the difference between the measured activity of commercial vials and the nominal one declared by the vendors. The multicenter study published by Gnesin *et al.* (2023) found that the activity assessed with PET underestimated by 21% for glass microspheres and overestimated by 15% for resin microspheres the vendor-calibrated activity while a good agreement between PET- and vendor-calibrated activities was found for a vials containing homogeneous ^{90}Y-chloride liquid solution. According to the results published by Auditore *et al.* (2023), this discrepancies can be attributed to the calibration factors used for measuring the activity of the vials at the vendor site. In particular, the trend of the microsphere to rapidly fall down to the bottom of the vial implies a measurement configuration quite different from the one used to retrieve the calibration factors with the YCl_3 solution. Moreover, also the geometry of the vial containing the microspheres showed to affect the measurements. Another relevant contribution comes from having neglected the emission of Internal Bremsstrahlung (IB) photons among the radioactive decay particles emitted by ^{90}Y (Auditore *et al.* 2023), a process usually not kept into account in activity estimation; nevertheless, recent studies confirmed its role in forming the signal registered by an activimeter (Auditore *et al.* 2021).

Aim of this study was to investigate, by means of Monte Carlo simulations, the several factors affecting the activity measurements and potentially responsible of the discrepancies discussed by Graves *et al.* (2022), Auditore *et al.* (2023), and Gnesin *et al.* (2023).

2. Materials and methods

The response of the Veenstra activity calibrator (Veenstra 2012) considered in this study was modelled by Monte Carlo (MC) simulations performed with GAMOS 6.0 (Arce *et al.* 2008, 2011), a user-friendly interface of the GEANT4 code (Agostinelli *et al.* 2003; Allison *et al.* 2006, 2016) extensively validated in the literature Arce *et al.* 2014. Three radioactive sources were considered: YCl_3, ^{90}Y-loaded glass and resin microspheres. The Veenstra activity calibrator, whose active volume was filled with pure argon at 14 bar of pressure, was reproduced according to the technical layouts provided by the vendor (Veenstra 2012). This MC setup was elsewhere validated (Auditore *et al.* 2021, 2022) and is shown in Fig. 1.

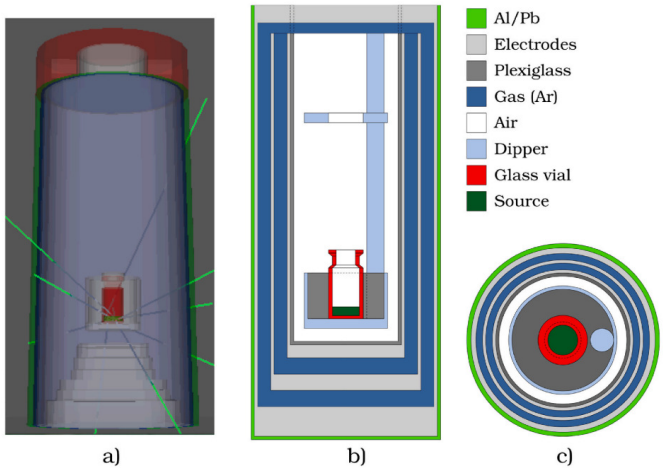

FIGURE 1. a): rendering of the geometry as reproduced by MC simulation together with particle tracks. b) and c): schematic 2D layouts of the experimental setup (not to scale) for the configuration including a plexiglass shield around the source) (Auditore *et al.* 2022).

The GmEMExtendedPhysics package, using by default the Livermore low-energy electromagnetic interaction models, including atomic de-excitation, was used; chemical compositions and densities of the considered materials were taken from the GEANT4 Database Material (Geant4 Collaboration 2024). The *RadioactiveDecay* class was used to simulate the beta-decay of ^{90}Y which does not include Internal Bremsstrahlung photon emission. To account for this process, further simulations were run in which photons were generated in the source volume with energy probabilities set in a user-defined file read by GAMOS and expressed as a constant-bin histogram, as explained in detail by (Auditore *et al.* 2021, 2022, 2023).

A range cut-off of 1 μm was used and 10^8 primary histories were simulated, to obtain MC estimates with relative statistical uncertainties of about 1%; no variance reduction technique was implemented. A workstation equipped with a 4th generation Intel Core i7 processor, was used to run simulations, each of which required about 1 h. YCl_3 was simulated as a 0.5 ml aqueous solution contained in a vial with standard geometry (the main

body of the vial is an hollow cylinder). ^{90}Y decays were uniformly generated in the solution. Results of this simulations were taken as the reference. ^{90}Y-loaded glass microspheres were simulated according to the scheme adopted by Auditore *et al.* (2023). The source was firstly simulated as a particulate solution in which microspheres are deposited to the bottom of the V-shaped vial, which is the one commercially used. The vial is shielded by a thick cylinder made of plexiglass that was also included in the MC simulations.

To estimate the influence of the distribution of microspheres in the vial, a second set of simulations was carried out considering the microsphere homogenously distributed in the aqueous solution. In this case the density of the whole solution was adjusted accordingly. Moreover, the commercial vial used to sell ^{90}Y-loaded glass microspheres is V-shaped having a thick base; the influence of the vial geometry was also studied. In all the simulation with ^{90}Y-loaded glass microspheres, the volume of the solution in the vial was set to 0.8 ml. The signals produced by the activity calibrator, in terms of electric current per activity unit (pA/MBq), estimated for the different configurations were compared with the reference, as described by Auditore *et al.* (2021). Similarly, ^{90}Y-loaded resin microspheres were firstly simulated at the bottom of a vial with cylindrical geometry. A further set of simulations was then carried out considering the microspheres uniformly distributed in the vial. Results were compared with the reference also in this case.

For each kind of microspheres, the comparison with the reference, YCl_3, is discussed in terms of relative percent difference $\varepsilon_{1,2}$, calculated as:

$$\varepsilon_{1,2} = 100 \cdot \frac{Y_{1,2} - Y_{YCl_3}}{Y_{YCl_3}}$$

where $\varepsilon_{1,2}$ refer to the real and modified configurations, respectively (see Auditore *et al.* 2021, Eq. 4).

3. Results and discussion

3.1. ^{90}Y-loaded glass microspheres. Results obtained for ^{90}Y-loaded glass microspheres are summarized in Table 1.

TABLE 1. Comparison between the signal estimated for YCl_3 and ^{90}Y-loaded glass microspheres in two configurations: (1) microspheres at the bottom of the V-shaped vial; (2) microspheres uniformly distributed in the V-shaped vial.

Source	YCl_3 (pA/MBq)	Glass microspheres (1) (pA/MBq)	ε_1 (%)	Glass microspheres (2) (pA/MBq)	ε_2 (%)
β	0.163	0.211	29.4	0.160	-1.8
γ_{IB}	0.024	0.020	-16.7	0.023	-4.2
$\beta + \gamma_{IB}$	0.187	0.231	23.5	0.184	-1.6

When considering the real distribution of microspheres in the vial (deposited at the vial bottom) and neglecting γ_{IB}, the signal registered by the activity calibrator differs from the one obtained with the YCl_3 reference solution by 29.4%. The difference reduces to -1.8%

when the microspheres are simulated uniformly distributed in the vial. These results indicate that if the microsphere were uniformly distributed in it (*e.g.*, by continuous stirring), the calibration factors deduced from the measurements of the activity of an YCl_3 solution could be used also for the ^{90}Y-loaded glass microspheres. Conversely, when considering the real microsphere distribution, a different calibration factor should be used. The inclusion of γ_{IB} as an additional source term in MC simulation reduces the discrepancy by 5.9% when the real distribution of the microspheres in the solution is considered and by 0.2% if the microspheres are homogeneously dispersed in the solution thus highlighting the role of γ_{IB} in such measurements.

The effect of the vial geometry was also investigated and the results are reported in Table 2.

TABLE 2. Comparison between the signal estimated for YCl_3 and ^{90}Y-loaded resin microspheres contained in a V-shaped (1) vial and in a vial with standard geometry (2).

Source	YCl_3 (pA/MBq)	Glass microspheres (1) (pA/MBq)	ε_1 (%)	Glass microspheres (2) (pA/MBq)	ε_2 (%)
β	0.163	0.211	29.4	0.197	20.8
γ_{IB}	0.024	0.020	-16.7	0.022	-8.3
$\beta + \gamma_{IB}$	0.187	0.231	23.5	0.218	16.6

There is evidence that the vial geometry affects the signal related to the beta emission of ^{90}Y (γ_{IB} are neglected) reducing the discrepancy with respect to the reference solution from 29.5% to 20.8%. Similarly, also the signal coming from γ_{IB} is affected by the vial geometry. Considering both beta emission and γ_{IB} the discrepancy with respect to the reference solution reduces from 23.5% to 16.6% when considering a cylindrical vial. Results for ^{90}Y-loaded glass microspheres are represented in Fig. 2.

TABLE 3. Comparison between the signal estimated for YCl_3 and ^{90}Y-loaded resin microspheres in two configurations: (1) microspheres at the bottom of the vial; (2) microspheres uniformly distributed in the vial.

Source	YCl_3 (pA/MBq)	Resin microspheres (1) (pA/MBq)	ε_1 (%)	Resin microspheres (2) (pA/MBq)	ε_2 (%)
β	0.163	0.135	-17.4	0.146	-10.4
γ_{IB}	0.024	0.024	0.0	0.025	4.2
$\beta + \gamma_{IB}$	0.187	0.159	-15.0	0.171	-8.6

3.2. ^{90}Y-loaded resin microspheres. Table 3 reports the MC simulation estimates for ^{90}Y-loaded resin microspheres. The discrepancy between the signal from the activimeter for YCl_3 and ^{90}Y-loaded resin microspheres reduces from -17.2% to -10.4% when considering the microspheres homogenously dispersed in the solution. The addition of γ_{IB} further

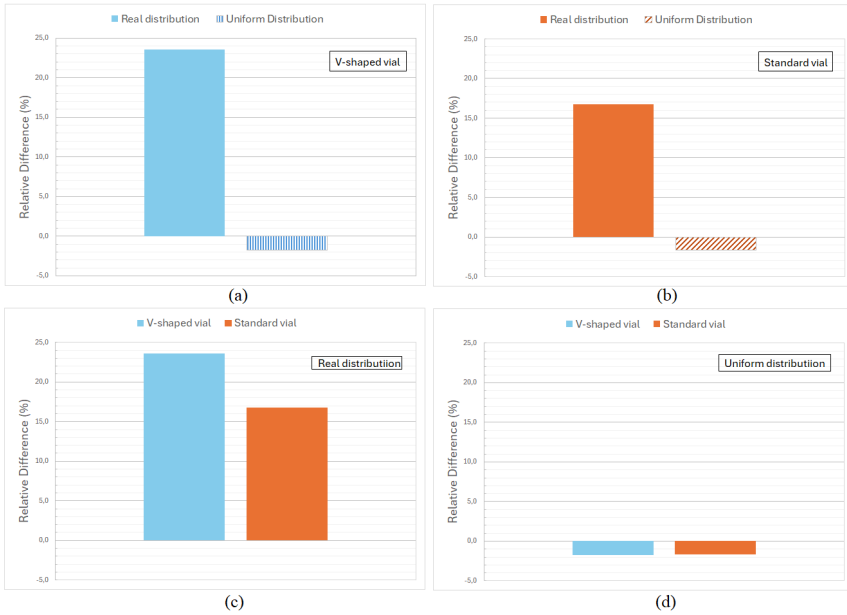

FIGURE 2. Relative percent difference between signals estimated for ^{90}Y-loaded glass microsperes respect to YCl_3: real vs uniform microsphere distribution for vials with V shape (a) and standard geometry (b); V-shaped *vs* standard vial geometry for real (c) and uniform (d) distribution.

reduces the discrepancy to -8.6%. Results are similar to those discussed for ^{90}Y-loaded glass microspheres and we can state that also for the measurement of the activity of resin microspheres the use of proper calibration factors is recommended.

4. Conclusions

In therapeutic Nuclear Medicine procedures, an accurate estimate of the administered activity is paramount to pursue the goal of safety and efficacy of the treatment. Recent studies highlighted important discrepancies in the determination of therapeutic activity of ^{90}Y-loaded glass and resin microspheres, devices widely used for TranArterial RadioEmbolization in the treatment of patients with HepatoCellular Carcinoma (HCC) and/or hepatic metastases, evidencing the importance of adopting proper calibration factors to get a realistic value of the activity. This study proves the dependence of the measurements on the real distribution of microspheres inside the vial as well as on the vial geometry, further suggesting the need to include, in the β-decay analysis, also the Internal Bremsstrahlung contribution to obtain reliable data.

Acknowledgments

D.P. acknowledges support from the PNRR - PNC ANTHEM project.

References

Agostinelli, S., Allison, J., Amako, K., Apostolakis, J., Araujo, H., Arce, P., Asai, M., Axen, D., Banerjee, S., Barrand, G., Behner, F., Bellagamba, L., Boudreau, J., Broglia, L., Brunengo, A., Burkhardt, H., Chauvie, S., Chuma, J., Chytracek, R., Cooperman, G., Cosmo, G., Degtyarenko, P., Dell'Acqua, A., Depaola, G., Dietrich, D., Enami, R., Feliciello, A., Ferguson, C., Fesefeldt, H., Folger, G., Foppiano, F., Forti, A., Garelli, S., Giani, S., Giannitrapani, R., Gibin, D., Gómez Cadenas, J., González, I., Gracia Abril, G., Greeniaus, G., Greiner, W., Grichine, V., Grossheim, A., Guatelli, S., Gumplinger, P., Hamatsu, R., Hashimoto, K., Hasui, H., Heikkinen, A., Howard, A., Ivanchenko, V., Johnson, A., Jones, F. W., Kallenbach, J., Kanaya, N., Kawabata, M., Kawabata, Y., Kawaguti, M., Kelner, S., Kent, P., Kimura, A., Kodama, T., Kokoulin, R., Kossov, M., Kurashige, H., Lamanna, E., Lampén, T., Lara, V., Lefebure, V., Lei, F., Liendl, M., Lockman, W., Longo, F., Magni, S., Maire, M., Medernach, E., Minamimoto, K., Mora de Freitas, P., Morita, Y., Murakami, K., Nagamatu, M., Nartallo, R., Nieminen, P., Nishimura, T., Ohtsubo, K., Okamura, M., O'Neale, S., Oohata, Y., Paech, K., Perl, J., Pfeiffer, A., Pia, M. G., Ranjard, F., Rybin, A., Sadilov, S., Di Salvo, E., Santin, G., Sasaki, T., Savvas, N., Sawada, Y., Scherer, S., Sei, S., Sirotenko, V., Smith, D., Starkov, N., Stoecker, H., Sulkimo, J., Takahata, M., Tanaka, S., Tcherniaev, E., Safai Tehrani, E., Tropeano, M., Truscott, P., Uno, H., Urban, L., Urban, P., Verderi, M., Walkden, A., Wander, W., Weber, H., Wellisch, J. P., Wenaus, T., Williams, D. C., Wright, D., Yamada, T., Yoshida, H., and Zschiesche, D. (2003). "Geant4 – a simulation toolkit". *Nuclear Instruments and Methods in Physics Research Section A: Accelerators, Spectrometers, Detectors and Associated Equipment* **506**(3), 250–303. DOI: 10.1016/S0168-9002(03)01368-8.

Allison, J., Amako, K., Apostolakis, J., Araujo, H., Dubois, P. A., Asai, M., Barrand, G., Capra, R., Chauvie, S., Chytracek, R., Cirrone, G. A. P., Cooperman, G., Cosmo, G., Cuttone, G., Daquino, G. G., Donszelmann, M., Dressel, M., Folger, G., Foppiano, F., Generowicz, J., Grichine, V., Guatelli, S., Gumplinger, P., Heikkinen, A., Hrivnacova, I., Howard, A., Incerti, S., Ivanchenko, V., Johnson, T., Jones, F., Koi, T., Kokoulin, R., Kossov, M., Kurashige, H., Lara, V., Larsson, S., Lei, F., Longo, F., Maire, M., Mantero, A., Mascialino, B., McLaren, I., Lorenzo, P. M., Minamimoto, K., Murakami, K., Nieminen, P., Pandola, L., Parlati, S., Peralta, L., Perl, J., Pfeiffer, A., Pia, M. G., Ribon, A., Rodrigues, P., Russo, G., Sadilov, S., Santin, G., Sasaki, T., Smith, D., Starkov, N., Tanaka, S., Tcherniaev, E., Tomé, B., Trindade, A., Truscott, P., Urban, L., Verderi, M., Walkden, A., Wellisch, J., Williams, D. C., Wright, D., Yoshida, H., and Peirgentili, M. (2006). "Geant4 developments and applications". *IEEE Transactions on Nuclear Science* **53**(1), 270–278. DOI: 10.1109/TNS.2006.869826.

Allison, J., Amako, K., Apostolakis, J., Arce, P., Asai, M., Aso, T., Bagli, E., Bagulya, A., Banerjee, S., Barrand, G., Beck, B. R., Bogdanov, A. G., Brandt, D., Brown, J. M. C., Burkhardt, H., Canal, P., Cano-Ott, D., Chauvie, S., Cho, K., Cirrone, G. A. P., Cooperman, G., Cortés-Giraldo, M. A., Cosmo, G., Cuttone, G., Depaola, G., Desorgher, L., Dong, X., Dotti, A., Elvira, V. D., Folger, G., Francis, Z., Galoyan, A., Garnier, L., Gayer, M., Genser, K. L., Grichine, V. M., Guatelli, S., Guèye, P., Gumplinger, P., Howard, A. S., Hřivnáčová, I., Hwang, S., Incerti, S., Ivanchenko, A., Ivanchenko, V. N., Jones, F. W., Jun, S. Y., Kaitaniemi, P., Karakatsanis, N., Karamitrosi, M., Kelsey, M., Kimura, A., Koi, T., Kurashige, H., Lechner, A., Lee, S. B., Longo, F., Maire, M., Mancusi, D., Mantero, A., Mendoza, E., Morgan, B., Murakami, K., Nikitina, T., Pandola, L., Paprocki, P., Perl, J., Petrović, I., Pia, M. G., Pokorski, W., Quesada, J. M., Raine, M., Reis, M. A., Ribon, A., Ristić Fira, A., Romano, F., Russo, G., Santin, G., Sasaki, T., Sawkey, D., Shin, J. I., Strakovsky, I. I., Taborda, A., Tanaka, S., Tomé, B., Toshito, T., Tran, H. N., Truscott, P. R., Urban, L., Uzhinsky, V., Verbeke, J. M., Verderi, M., Wendt, B. L., Wenzel, H., Wright, D. H., Wright, D. M., Yamashita, T., Yarba, J., and Yoshida, H. (2016). "Recent developments in Geant4".

Nuclear Instruments and Methods in Physics Research Section A: Accelerators, Spectrometers, Detectors and Associated Equipment **835**, 186–225. DOI: 10.1016/j.nima.2016.06.125.

Amato, E., Auditore, L., Italiano, A., Pistone, D., Arce, P., Campenní, A., and Baldari, S. (2020). "Full Monte Carlo internal dosimetry in nuclear medicine by means of GAMOS". *Journal of Physics: Conference Series* **1561**, 012002. DOI: 10.1088/1742-6596/1561/1/012002.

Arce, P., Ignacio Lagares, J., Harkness, L., Pérez-Astudillo, D., Cañadas, M., Rato, P., De Prado, M., Abreu, Y., De Lorenzo, G., Kolstein, M., and Díaz, A. (2014). "GAMOS: A framework to do GEANT4 simulations in different physics fields with an user-friendly interface". *Nuclear Instruments and Methods in Physics Research Section A: Accelerators, Spectrometers, Detectors and Associated Equipment* **735**, 304–313. DOI: 10.1016/j.nima.2013.09.036.

Arce, P., Lagares, J. I., Harkness, L., Desorgher, L., Lorenzo, G. de, Abreu, Y., and Wang, Z. (2011). "GAMOS: An easy and flexible way to use GEANT4". In: *2011 IEEE Nuclear Science Symposium Conference Record*, pp. 2230–2237. DOI: 10.1109/NSSMIC.2011.6154455.

Arce, P., Rato, P., Cañadas, M., and Lagares, J. I. (2008). "GAMOS: A Geant4-based easy and flexible framework for nuclear medicine applications". In: *2008 IEEE Nuclear Science Symposium Conference Record*, pp. 3162–3168. DOI: 10.1109/NSSMIC.2008.4775023.

Auditore, L., Amato, E., Boughdad, S., Meyer, M., Testart, N., Cicone, F., Beigelman-Aubry, C., Prior, J. O., Schaefer, N., and Gnesin, S. (2020). "Monte Carlo ^{90}Y PET/CT dosimetry of unexpected focal radiation-induced lung damage after hepatic radioembolisation". *Physics in Medicine and Biology* **65**(23), 235014. DOI: 10.1088/1361-6560/abbc80.

Auditore, L., Amato, E., Italiano, A., Arce, P., Campenní, A., and Baldari, S. (2019). "Internal dosimetry for TARE therapies by means of GAMOS Monte Carlo simulations". *Physica Medica* **64**, 245–251. DOI: 10.1016/j.ejmp.2019.07.024.

Auditore, L., Juget, F., Italiano, A., Pistone, D., Nedjadi, Y., Gnesin, S., and Amato, E. (2021). "Relevance of Internal Bremsstrahlung photons from ^{90}Y decay: an experimental and Monte Carlo study". *Physica Medica* **90**, 158–163. DOI: 10.1016/j.ejmp.2021.10.006.

Auditore, L., Pistone, D., Amato, E., and Italiano, A. (2022). "Monte Carlo Methods in Nuclear Medicine". In: *Nuclear Medicine and Molecular Imaging*. Ed. by A. Signore. Vol. 1. Oxford: Elsevier, pp. 587–606. DOI: 10.1016/B978-0-12-822960-6.00136-8.

Auditore, L., Pistone, D., Italiano, A., Amato, E., and Gnesin, S. (2023). "Monte Carlo simulations corroborate PET-measured discrepancies in activity assessments of commercial ^{90}Y vials". *The Journal of Nuclear Medicine* **64**(9), 1471–1477. DOI: 10.2967/jnumed.123.265494.

Chiesa, C., Sjogreen-Gleisner, K., Walrand, S., Strigari, L., Flux, G., Gear, J., Stokke, C., Gabina, P. M., Bernhardt, P., and Konijnenberg, M. (2021). "EANM dosimetry committee series on standard operational procedures: a unified methodology for ^{99m}Tc-MAA pre- and ^{90}Y peri-therapy dosimetry in liver radioembolization with ^{90}Y microspheres". *EJNMMI Physics* **8**(1), 77. DOI: 10.1186/s40658-021-00394-3.

Geant4 Collaboration (2024). *User's Guide for Application Developers - Appendix*. Last accessed: 2024-06-06. URL: https://geant4-userdoc.web.cern.ch/UsersGuides/ForApplicationDeveloper/html/Appendix/appendix.html.

Gnesin, S., Mikell, J. K., Conti, M., Prior, J. O., Carlier, T., Lima, T. V. M., and Dewaraja, Y. K. (2023). "A multicenter study on observed discrepancies between vendor-stated and PET-measured ^{90}Y activities for both glass and resin microsphere devices". *The Journal of Nuclear Medicine* **64**(5), 825–828. DOI: 10.2967/jnumed.122.264458.

Graves, S. A., Martin, M., Tiwari, A., Merrick, M., and Sunderland, J. (2022). "SIR-Spheres activity measurements reveal systematic miscalibration". *The Journal of Nuclear Medicine* **63**(8), 1131–1135. DOI: 10.2967/jnumed.121.262650.

Levillain, H., Bagni, O., Deroose, C. M., Dieudonné, A., Gnesin, S., Grosser, O. S., Kappadath, S. C., Kennedy, A., Kokabi, N., Liu, D. M., Madoff, D. C., Mahvash, A., Martinez de la Cuesta, A., Ng,

D. C. E., Paprottka, P. M., Pettinato, C., Rodríguez-Fraile, M., Salem, R., Sangro, B., Strigari, L., Sze, D. Y., de Wit van der veen, B. J., and Flamen, P. (2021). "International recommendations for personalised selective internal radiation therapy of primary and metastatic liver diseases with yttrium-90 resin microspheres". *European Journal of Nuclear Medicine and Molecular Imaging* **48**(5), 1570–1584. DOI: 10.1007/s00259-020-05163-5.

Pistone, D., Italiano, A., Auditore, L., Mandaglio, G., Campenní, A., Baldari, S., and Amato, E. (2022). "Relevance of artefacts in ^{99m}Tc-MAA SPECT scans on pre-therapy patient-specific ^{90}Y TARE internal dosimetry: A GATE Monte Carlo study". *Physics in Medicine and Biology* **67**(11), 115002. DOI: 10.1088/1361-6560/ac6b0f.

Veenstra (2012). *VEENSTRA VDC-405 Ionization Chamber Datasheet, Comecer*. (Private Document).

Weber, M., Lam, M., Chiesa, C., Konijnenberg, M., Cremonesi, M., Flamen, P., Gnesin, S., Bodei, L., Kracmerova, T., Luster, M., Garin, E., and Herrmann, K. (2022). "EANM procedure guideline for the treatment of liver cancer and liver metastases with intra-arterial radioactive compounds". *European Journal of Nuclear Medicine and Molecular Imaging* **49**(5), 1682–1699. DOI: 10.1007/s00259-021-05600-z.

[a] Università degli Studi di Messina,
Dipartimento di Scienze Biomediche, Odontoiatriche e delle Immagini Morfologiche e Funzionali,
Messina, Italy

[b] Istituto Nazionale di Fisica Nucleare,
Sezione di Catania,
Catania, Italy

[c] Institute of Radiation Physics, Lausanne University Hospital and University of Lausanne,
Lausanne, Switzerland,

[d] Università degli Studi di Messina,
Dipartimento di Scienze Matematiche e Informatiche, Scienze Fisiche e Scienze della Terra,
Messina, Italy

[e] Università degli Studi della Campania "Luigi Vanvitelli",
Dipartimento di Matematica e Fisica,
Caserta, Italy

[f] Istituto Nazionale di Fisica Nucleare,
Sezione di Napoli,
Napoli, Italy

[g] Azienda Ospedaliera Universitaria "Gaetano Martino",
Unità di Fisica Sanitaria,
Messina, Italy

[*] To whom correspondence should be addressed | email: antonio.italiano@ct.infn.it

Communicated 6 May 2024; manuscript received 1 July 2024; published online 12 November 2024